

**Investigation on rail corrugation grinding criterion based on coupled vehicle–track dynamics and rolling contact fatigue model**

Liang, Hongqin; Li, Wei; Zhou, Zhijun; Wen, Zefeng; Li, Shaoguang; An, Dong

**DOI**

[10.1177/1077546321989201](https://doi.org/10.1177/1077546321989201)

**Publication date**

2021

**Document Version**

Final published version

**Published in**

JVC/Journal of Vibration and Control

**Citation (APA)**

Liang, H., Li, W., Zhou, Z., Wen, Z., Li, S., & An, D. (2021). Investigation on rail corrugation grinding criterion based on coupled vehicle–track dynamics and rolling contact fatigue model. *JVC/Journal of Vibration and Control*, 28(9-10), 1176-1186. <https://doi.org/10.1177/1077546321989201>

**Important note**

To cite this publication, please use the final published version (if applicable). Please check the document version above.

**Copyright**

Other than for strictly personal use, it is not permitted to download, forward or distribute the text or part of it, without the consent of the author(s) and/or copyright holder(s), unless the work is under an open content license such as Creative Commons.

**Takedown policy**

Please contact us and provide details if you believe this document breaches copyrights. We will remove access to the work immediately and investigate your claim.

***Green Open Access added to TU Delft Institutional Repository***

***'You share, we take care!' - Taverne project***

**<https://www.openaccess.nl/en/you-share-we-take-care>**

Otherwise as indicated in the copyright section: the publisher is the copyright holder of this work and the author uses the Dutch legislation to make this work public.

# Investigation on rail corrugation grinding criterion based on coupled vehicle–track dynamics and rolling contact fatigue model

Hongqin Liang<sup>1</sup> , Wei Li<sup>2</sup>, Zhijun Zhou<sup>2</sup>, Zefeng Wen<sup>2</sup>, Shaoguang Li<sup>3</sup> and Dong An<sup>1</sup>

Journal of Vibration and Control  
2021, Vol. 0(0) 1–11  
© The Author(s) 2021  
Article reuse guidelines:  
[sagepub.com/journals-permissions](https://sagepub.com/journals-permissions)  
DOI: 10.1177/1077546321989201  
[journals.sagepub.com/home/jvc](https://journals.sagepub.com/home/jvc)  


## Abstract

Based on the measured spectra of rail roughness and track structures longitudinal roughness, the rail grinding limit is studied with the help of an established coupled dynamic metro vehicle–track model and a rolling contact fatigue model. The results indicate that metro rail grinding control should be regulated according to corrugation wavelength range and operating speed. Based on the rolling contact fatigue model, longer wavelength of rail corrugation has less influence on the wheel rolling contact fatigue. For the metro lines with a maximum operating speed of 80 km/h, the average levels of rail corrugation in the wavelength ranges of 30–65 mm, 65–125 mm, and 125–250 mm should be less than 5.4, 24.8, and 33.8 dB re 1  $\mu\text{m}$ , respectively; for the ones with the operating speed of 80–120 km/h, the corresponding average corrugation levels in the three wavelength ranges should be less than 4.4, 9.8, and 29.8 dB re 1  $\mu\text{m}$ , respectively.

## Keywords

Metro rail corrugation, rolling contact fatigue, vehicle–track model, corrugation limit, grinding

## 1. Introduction

With the fast development of metro rail system, the wheel–rail rolling contact fatigue becomes more and more concerned, especially with rail corrugation problems (Ekberg et al., 2002; Li et al., 2016). Rail corrugation not only accelerates the wheel–rail dynamic interactions which lead to the vehicle–track system failures and ground and building vibrations (Auersch, 2020) but also reduces the ride comfort and poses some threats to train safe operation.

Much research has been conducted to explain the corrugation mechanism because its existence (Jin et al., 2005, 2016; Li et al., 2017) and many countermeasures against rail corrugation were proposed, such as replacements with head-hardened rail materials (Heyder and Girsch, 2005) and rail fastener (Jin et al., 2016), application of frictional modifier (Eadie et al., 2002, 2008; Eadie and Santoro, 2006), mounting vibrations absorbing dampers on vehicle and track systems (Christophe et al., 2009; Grassie and Elkins, 1998; Wu, 2011), variation of train speeds (Batten et al., 2011; Bellette et al., 2008; Meehan et al., 2009), and etc. In Grassie and Kalousek (1993), Grassie (2009) reviewed previous research progresses on different corrugations and correspondingly different remedies. By improving the rail material hardness, the wear resistance increases and the corrugation development therefore decreases, except for

the increasing wear of the wheelset. This approach is widely used in railway industry for corrugation reduction (Grassie and Kalousek, 1993; Heyder and Girsch, 2005). The application of frictional modifiers against corrugation was discussed in Eadie et al. (2002); Eadie and Santoro (2006); Eadie et al. (2008). With the friction modifier, friction coefficient between wheel–rail contact can be controlled within 0.3–0.4, and this reduction in friction coefficient can lessen the wear because of frictional rolling contact. Wheelset dampers can be effective to the corrugation caused by the wheelset torsional vibrations (Grassie and Elkins, 1998; Christophe et al., 2009), whereas the implementation is actually difficult because of the limited

<sup>1</sup>School of Mechanical Engineering, Southwest Jiaotong University, China

<sup>2</sup>State Key Laboratory of Traction Power, Southwest Jiaotong University, China

<sup>3</sup>Faculty of Civil Engineering and Geosciences, Delft University of Technology, The Netherlands

Received: 22 September 2020; accepted: 12 December 2020

### Corresponding author:

Hongqin Liang, School of Mechanical Engineering, Southwest Jiaotong University, No. 111, First Section, North of Second Ring Road, Chengdu 610031, China.

Email: [hongqinliang@swjtu.edu.cn](mailto:hongqinliang@swjtu.edu.cn)

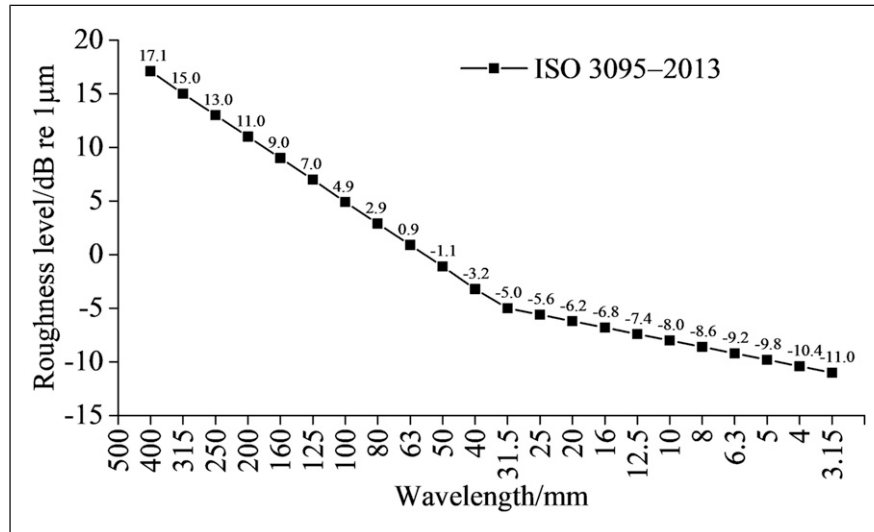


**Figure 1.** 1/3 octave spectrum of ISO 3095, 2013, for rail roughness (20).

space of the bogie and for this reason, it is usually necessary to redesign the wheelset. With numerical analysis, Wu (2011) found that the installation of rail dampers at rail web can suppress pinned–pinned corrugation. Variation of train speeds is another approach to control the corrugation. This was theoretically confirmed that the uniformity in train speed will increase the corrugation growth rate (Batten et al., 2011; Bellette et al., 2008; Meehan et al., 2009). To solve the corrugation problem, the train operation speed needs to be varied, whereas in practice, this is difficult to realize.

Currently, grinding is the most popular and effective way to reduce corrugation and the only way to completely get the corrugation geometrically removed. Besides, preventive grinding is effective to postpone the corrugation formation, for example, for five years (Guidat, 1996). There has been no generally accepted standard concerning the rail grinding. Some countries conduct rail grinding maintenance from the consideration of train safe operation, others from the grinding introduced damages to wheel–rail materials, whereas some others from the consideration of controlling corrugation induced vibration noise. German Railway (DB) and Danish railway (DSB) investigated rail grinding based on vibration noise mainly based on allowable rail corrugation severity defined by EN ISO 3095–2013 (2013). This grinding criterion on roughness levels increases the maintenance cost for the metro rail system. To optimize the grinding maintenance, that is, on the one hand to reduce the grinding cost, and on the other hand to make a more reasonable grinding schedule, it is necessary to propose a regulation on rail grinding which is applicable to different corrugations. To this end, the study investigates from the aspect of rolling contact fatigue of wheel–rail materials on corrugation grinding tolerance.

**Table 1.** Limits of corrugation magnitude and acceptance criteria for rail longitudinal roughness based on allowable ratios.

Wavelength range (mm)	10–30	30–100	100–300	300–1000
Grinding quality: level 1	5%	5%	5%	5%
Grinding quality: level 2	–	10%	10%	–
Amplitude (mm)	±0.010	±0.010	±0.015	±0.075

## 2. Rail corrugation grinding criterion

Currently, there are no general standards available on corrugation limit control. This could be inherently because of the complexity of the track system and actual different train operation situations. Specifically, high-speed railway, normal lines, heavy haul railway, and metro rail system have different operating speeds, curve radii, axle loads, vehicle suspensions, and track structures. Second, it is also because of different characteristics of corrugations. Moreover, it is related to the different tolerances from different infra managers on the corrugations, such as the corrugation noise is of special concern to DB, whereas in some Chinese railways, maintenances are conducted based on the running safety influenced by rail corrugation. Inspection methods on rail corrugation can be referenced to as in (EN 15,610:2009, 2009).

So far, standards on the corrugation limit are evaluated by the noise emission level, for example, ISO 3095–2013 (2013) (see Figure 1). For roughness in the wavelength range of 10–80 mm, the standard defines that the roughness level exceeds the limit when the corrugation peak of a single wavelength in one-third octave is higher than 6 dB, or corrugation peaks of three consecutive wavelengths exceed 3 dB.

The standard on corrugation grinding quality is evaluated by some parameters of ground rails. The acceptance level for rail corrugation grinding is defined in EN 13231–3:

**Table 2.** Acceptance standards for rail corrugation grinding operation.

Items	Acceptance criteria				Measurement methods	Explanations
Wavelength (mm)	10–30	30–100	100–300	300–1000		
Sampling window size(mm)	600	600	1000	5000		
Average of troughs depth (mm)	0.02	0.02	0.03	0.15	Measurement accuracy up to 0.01 mm	Within 8 days after grinding or the gross tonnage smaller than 0.3 Million Gross Ton
					Measurement length not smaller than sampling window size	
					Continuous measurement of	
Percentage of allowable surplus (%)	5%	5%	5%	5%	Continuous measurement of 100 m (vehicle measurement) or 30 m (hand measurement) ground rail	

2012 (2012) (see Table 1). According to the definition, the acceptance of corrugation grinding maintenance is fulfilled when the amplitudes of corrugations of different wavelengths do not exceed the corresponding quality tolerance ratios. For instance, for the corrugation with wavelength of 10–30 mm, if less than 5% of the number of amplitudes is within  $\pm 0.01$  mm, it is defined as the highest grinding quality. Besides, the evaluation on corrugation grinding quality should be done immediately after the grinding maintenance, or should be less than eight days after the grinding, or the total wheel loads because the grinding should not be larger than 0.3 Million Gross Ton.

With the development of Chinese railways, there are also relevant standards to evaluate corrugation grinding and acceptance criterion. In “railway maintenance regulations” (Railway Transport, 2006), it states that when the vehicle operation speed is lower than 120 km/h, corrugation with valley depth larger than 0.5 mm is defined as slight damage of rail; when the speed is higher than 120 km/h, corrugation with valley depth larger than 0.3 mm is slight damage of rail. It also defines the rail grinding acceptance criterion that the depth of corrugation valley should be smaller than 0.2 mm measured with a 1-m straight ruler. In addition, Chinese railway industrial standard TB/T 2658.22 (2010) defines the grinding criterion of grinding vehicles on normal tracks and at switches and crossings. Specifically, the corrugation valley depths after grinding should be less than 0.04 mm when the wavelength is in the range of 30–300 mm and less than 0.2 mm within 300–1000 mm.

In the “management methods on high-speed railway grinding” (General Railway Transport, 2014), it emphasizes the rail corrugation as one type of rail defects to be controlled. Specifically, for high-speed railways with the speed of 200–350 km/h, the average corrugation valley depth should not exceed 0.04 mm (with vehicle-borne loaded measurement), or 0.08 mm with portable measurement equipment, and the wavelength should not be larger than 300 mm. It also defines the acceptance standard of corrugation grinding, as shown in Table 2.

Different corrugation wavelengths determine the corresponding frequency vibrations they can excite. Short pitch corrugation excites higher frequency wheel–rail vibrations, which lead to not only the noise radiation, but also the accelerating fatigue failures of vehicle–track components. Long-wavelength corrugation mainly contributes to low-frequency vibrations. The vibrations are transferred to the track and ground vibrations in the end, causing problems to the track settlement and the nearby structures. Therefore, different corrugations should be treated with different countermeasures. Currently, there is little research on material fatigues caused by rail corrugation. Nielsen and Ekberg (2011) analyzed the corrugation acceptance criteria based on the wheel–rail rolling contact fatigues and rolling noise. They studied the influences of different corrugations under different train speeds on the passenger and freight trains wheel–rail rolling contact noise and the subsurface material rolling contact fatigue parameters. Regarding to the passenger vehicles, the risk on the wheel subsurface material rolling contact fatigue cracks initiation from rail corrugation is minor, except for corrugation on a severe stage. Short pitch corrugation brings considerable influences on both freight and passenger trains rolling noise. With the train speed increase, the control on rail corrugation becomes even more important. This study will investigate the grinding limit from the perspective of wheel–rail material rolling contact fatigue because of rail corrugation.

The wheel–rail contact forces can be measured through the static calibration, that is, low-pass filtering of the measured force signals (TB/T 2489–94, 1995), whereas a deficiency of the method is that it cannot capture the dynamic contact force excited by wheel–rail surface roughness. In China, the wheel–rail contact force is measured with an instrumented wheelset (TB/T 2360–93, 1994). The upper frequency that it measures is smaller than 100 Hz, and this is not sufficient to obtain the high-frequency wheel–rail contact forces from short pitch corrugation. Gullers et al. (2008) investigated the instrumented

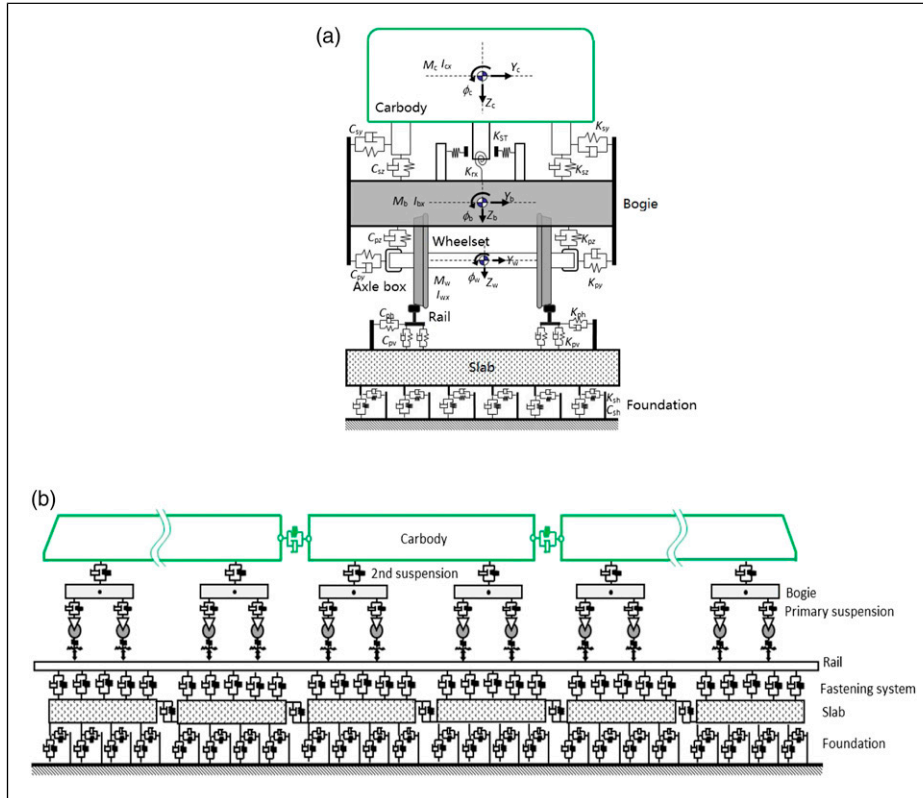


**Figure 2.** Couple metro vehicle–track dynamic model (Li, 2015). (a) Coupled vehicle–track model (front view) and (b) coupled vehicle–track model (side view).

wheelset under high-frequency excitation, and analyzed the in situ measured high-frequency contact forces. This study mainly studies the dynamic wheel–rail contact forces under high-frequency excitations with short pitch corrugation through a coupled metro vehicle–track dynamic model.

### 3. Rail grinding limit based on wheel–rail rolling contact fatigue

#### 3.1. Coupled metro vehicle–track dynamic model

Based on vehicle–track coupled dynamics theory (Xu and Zhai, 2020; Zhai, 2020), Timoshenko theory and finite element analysis, a coupled metro vehicle–track dynamic model was developed. The model of the vehicle consists of six cars, and each car is simplified with a car body, two bogies, four wheelsets, and eight axle boxes which are treated as multi-rigid body system. Each car body, bogie, and wheelset includes six degrees of freedom, that is, longitudinal, lateral, vertical, pitch, roll, and spin motions. Fourdegrees of freedom of longitudinal, lateral, roll, and pitch are considered for the axle box. Hence, the total degree of freedom of the vehicle–track system is 74. The primary and secondary suspensions are simplified as spring–damper elements in the vertical and lateral directions. The track

system consists of two rails, fastening system, track bed, and subgrade. Two rails, treated as the Timoshenko beam, are discretely supported, with consideration of vertical, lateral, and torsional vibrations. The length of the rail is set to 250 m. The two ends of the rail are hinged. The slab layer is modeled as 3D solid element. The total number of track slabs considered in the track model is 20. In the FE model for the track slabs, each slab consists of 1845 nodes and 1120 3D solid hexahedron elements. The dimension of the slab is  $12.5 \times 2.41 \times 0.29 \text{ m}^3$ . The Young's modulus and density of the slab are 39.0 GPa and  $2500 \text{ kg/m}^3$ , respectively. To reduce the required computational effort efficiently, the modal superposition method is adopted to solve the equations of motion of the slabs. This method can be used to decouple the FE equations of motion of slab nodes (Li, 2015).The fastening system, the foundation below the slab layer, and the connection between adjacent slab blocks are modeled as spring–damper elements as shown in Figure 2.

#### 3.2. Measurement and evaluation on corrugation

To analyze the influence of corrugation on wheel–rail rolling contact fatigue, the corrugation severity is evaluated by the roughness level. The rail roughness level is

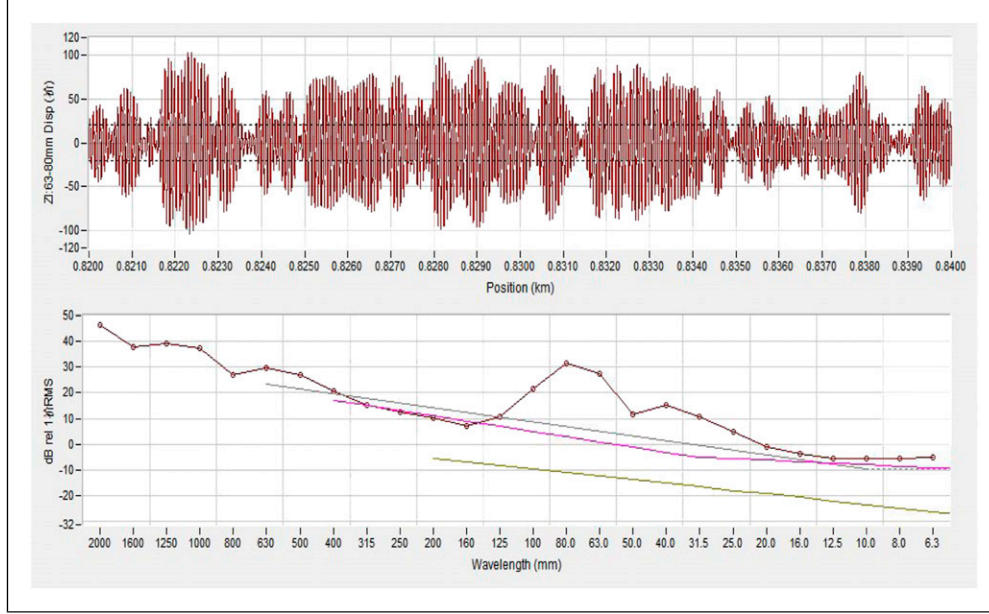


**Figure 3.** Rail roughness obtained from field measurement.

measured with a corrugation analysis trolley (CAT) (Grassie et al., 1999). The technique is widely used because of its high accuracy.

According to EN ISO 3095–2013 (2013), the rail surface roughness level is defined as

$$L_r = 10 \times \log_{10} \left( \frac{\tilde{r}^2}{\tilde{r}_{\text{ref}}^2} \right) (\text{dB re } 1 \mu\text{m}) \quad (1)$$

where  $L_r$  is the rail surface roughness level, dB,  $\tilde{r}$  the root mean square (RMS) value,  $\mu\text{m}$ ,  $\tilde{r}_{\text{ref}}$  the reference roughness and  $\tilde{r}_{\text{ref}} = 1 \mu\text{m}$ .

The corrugation severity of different wavelengths is represented with roughness levels at different wavelength bands (Nielsen and Ekberg, 2011).

The RMS of corrugation is evaluated at each wavelength band (evaluated in one-third octave bands), for example, the RMS of corrugation in the wavelength range of 30–65 mm (including wavelengths of 31.6 mm, 40 mm, 50 mm, and 63 mm) is

$$r_{\text{mean},30-65 \text{ mm}}^2 = r_0^2 \frac{1}{4} \sum_{i=1}^4 10L_{r,i}/10 \quad (2)$$

$$L_{r,30-65 \text{ mm}} = 10 \log_{10} \left( \frac{r_{\text{mean},30-65 \text{ mm}}^2}{r_0^2} \right) \quad (3)$$

Based on the in situ measured data, corrugation is reproduced by overlapping a group of sinusoidal functions. The detailed method is: (1) rail roughness levels,  $L_{r,i}$ , are obtained with measurement; (2) the rail roughness in the

spatial domain is reproduced with a group of sinusoidal functions based on (Hiensch, 2002)

$$r(x) = \sum_{i=1}^M a_i \left[ \sum_{j=1}^N \sin \left( \frac{2\pi}{\lambda_{ij}} x + \phi_{ij} \right) \right] \quad (4)$$

where  $r(x)$  is the corrugation amplitudes in the longitudinal direction,  $M$  is the number of wavelength bands in the corrugation,  $N$  is the number of sinusoidal cycles of each wavelength band,  $a_i$  is the amplitude of the corrugation expressed as sinusoidal function in each band,  $\lambda_{ij}$  is the corrugation wavelength, and  $\phi_{ij}$  is the phase angle ( $\phi_{ij} \in 0-2\pi$ ).

In each wavelength band, assuming the number of waves increases with a constant value of  $\Delta\kappa_i$ ,  $\Delta\kappa$  is determined by the maximum and minimum wavelength within the wavelength band

$$\Delta\kappa_i = \frac{2\pi}{N} \left( \frac{1}{\lambda_{i,\text{min}}} - \frac{1}{\lambda_{i,\text{max}}} \right) \quad (5)$$

Hence, the amplitude in each wavelength band based on (1) is

$$a_i = \sqrt{\frac{2}{N}} \times 10^{L_{r,i}/20} \quad (6)$$

Figure 3 shows a 20-m rail roughness measurement by CAT in spatial domain and wavelength domain. The main wavelength component is from 63–80 mm. The measured roughness is 63–80-mm band-pass filtered and reproduced based on equation (4). This is shown in Figure 4. The comparison of them shows that the maximum difference is

not larger than 0.2 mm. Hence, the corrugation from equation (4) can approximately reflect the actual corrugation situation.

### 3.3. Theory on rolling contact fatigue

To analyze the wheel material fatigue state under wheel–rail rolling contact, the equivalent Dang Van stress of wheel subsurface material is used to determine whether the rolling contact fatigue crack initiates. It is expressed as (Ekberg et al., 2002)

$$FI_{\text{sub}} = \frac{F_z}{4\pi ab} (1 + \mu^2) + \alpha_{DV} \sigma_{h,\text{res}} \quad (7)$$

where  $F_z$  is the wheel–rail vertical contact force,  $a$  and  $b$  are the semi-contact axis in longitudinal and lateral directions,  $\alpha_{DV}$  is a material parameter, and  $\sigma_{h,\text{res}}$  is the average of

residual stresses (hydrostatic stress, shown as positive values when materials are under extension).

As the residual stresses of wheel subsurface materials after the wheel passage are under compression,  $\alpha_{DV}$  and  $\sigma_{h,\text{res}}$  are negative values, and they reduce wheel material equivalent stresses. However, the beneficial influence under a rolling wheel does not exist (Desimone et al., 2006). Therefore, the value of  $\sigma_{h,\text{res}}$  is assumed to be 0 (ISO 3095–2013, 2013). When the fatigue parameter  $FI_{\text{sub}}$  exceeds the material fatigue limit, cracks begin to initiate. Considering the manufacturing flaws, the material fatigue limit stress should be to some extent smaller than the nominal value. In this study, the value is set to be 220 MPa from (Ekberg et al., 2002; ISO 3095–2013, 2013). According to Ekberg et al. (2002), the maximum shear stresses, and hence fatigue cracks and wear, appear at the contact surface when the friction coefficient is larger than 0.3, and in the subsurface

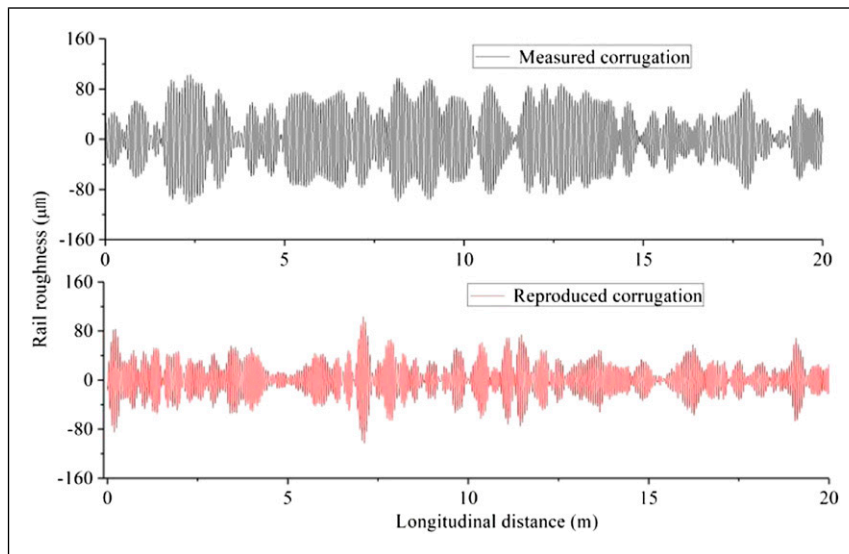


**Figure 4.** Comparison of rail roughness status between field measured corrugation and reproduced corrugation.

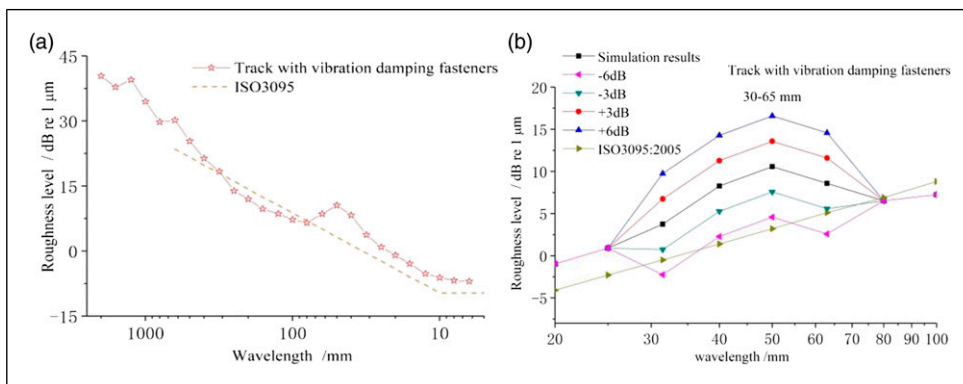


**Figure 5.** 1/3 octave spectrum of rail roughness of wavelength 30–65 mm (with reference to track of damping type fastener). (a) Field test roughness spectrum and (b) spectrograms in test range.

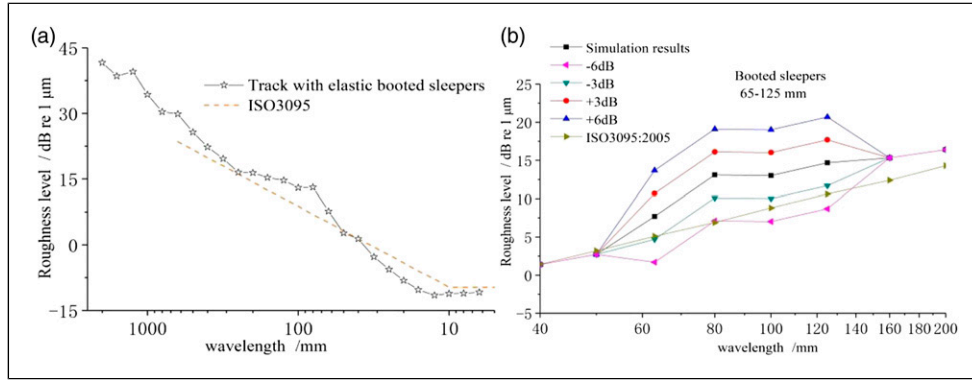


**Figure 6.** 1/3 octave spectrum of rail roughness of wavelength 65–125 mm (with reference to track of damping type fastener). (a) Field test roughness spectrum and (b) spectrograms in test range.

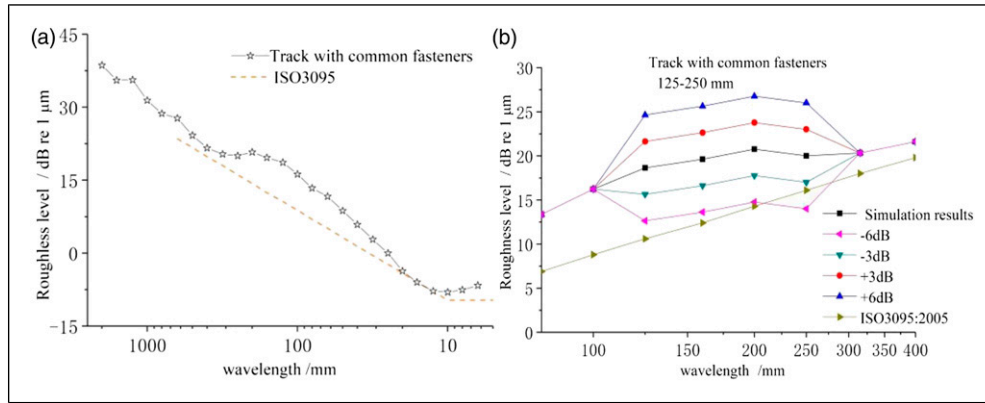


**Figure 7.** 1/3 octave spectrum of rail roughness of wavelength 125–250 mm (with reference to track of damping type fastener). (a) Field test roughness spectrum and (b) spectrograms in test range.

when the friction coefficient is smaller than 0.3 mm. This study considers the latter situation that the friction coefficient is smaller than 0.3.

#### 4. Rail roughness measurement and rolling contact fatigue analysis

To represent the rail roughness levels in general, the measured roughness spectra from railway track with the vibration attenuation fastening system, normal fastening systems and with booted sleepers, and normal fastening systems (Li, 2015) are averaged to get the roughness level of different wavelengths and from different track scenarios.

Based on current field measured corrugation data (Li, 2015), typical corrugation wavelengths corresponding to railway track with vibration attenuation fastening system, normal fastening system with booted sleepers, and normal fastening system are 30–65 mm, 65–125 mm, and 125–250 mm. One-third octave spectra of the corrugation in the corresponding three wavelength ranges are separately illustrated in Figure 5–7. Based on equation (2), the rail

roughness levels of corrugations in the three bands are 8.4, 12.8, and 19.8 dB re  $1 \mu\text{m}$ .

Hereinafter, the wheel–rail contact fatigue is analyzed at several wavelength bands. First, the roughness level (or corrugation) is derived from the field measurement. It is input to the coupled metro vehicle–track dynamic model to obtain the contact patches and vertical contact forces in the presence of corrugation. Figures 8 and 9 show the simulated vertical wheel–rail contact forces and the semi-axis of the contact patch which are the contact radii  $a$  and  $b$  of the contact ellipse with the rail roughness of wavelength 30–65 mm. Finally, the wheel–rail contact fatigues parameters are derived from equation (7).

Table 3 lists the maximum fatigue parameters and the percentage of which exceeds 220 MPa when the front bogie is passing over the corrugated zone (with a running distance of 40 m) with a corrugation wavelength of 30–65 mm under different speeds. The corrugation profile input to the model is the measured profile as shown in Figure 5(a). From the figure, it is seen that the fatigues parameters of the first wheelset are slightly larger than that of the second wheelset,

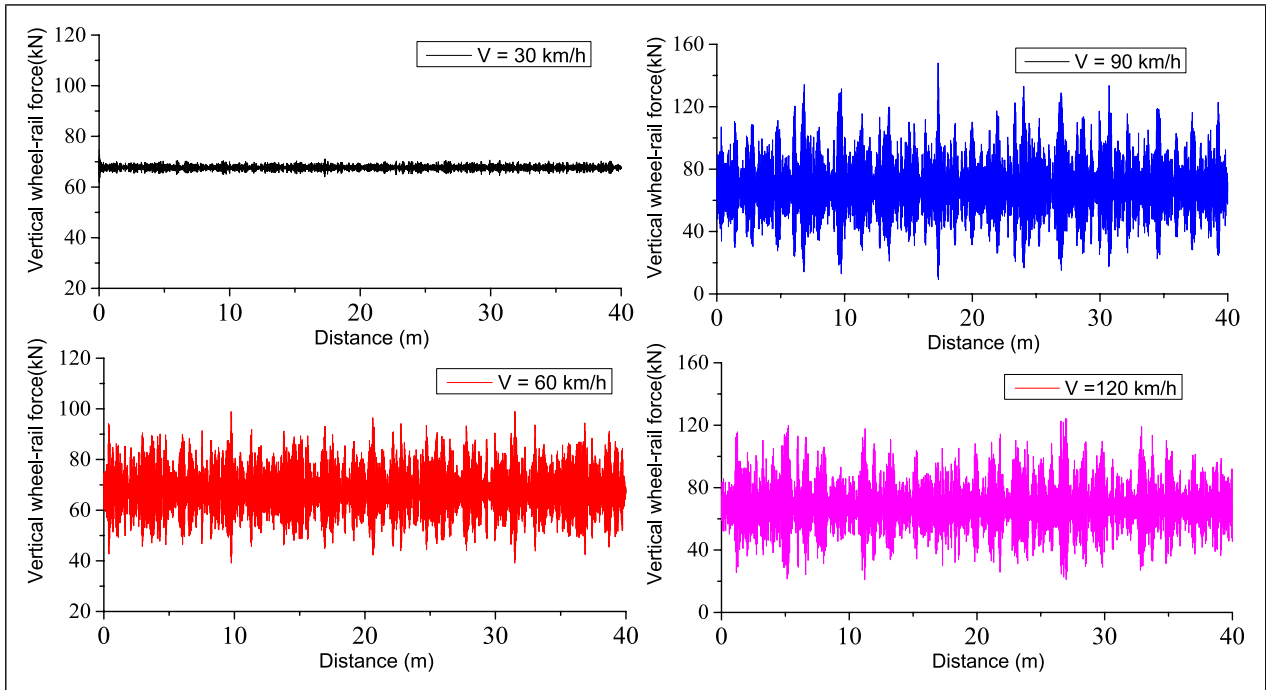


**Figure 8.** Vertical wheel–rail force calculated by the vehicle–track dynamic model when the wheel–rail system was excited by field tested rail irregularity with wavelength of 30–65 mm.

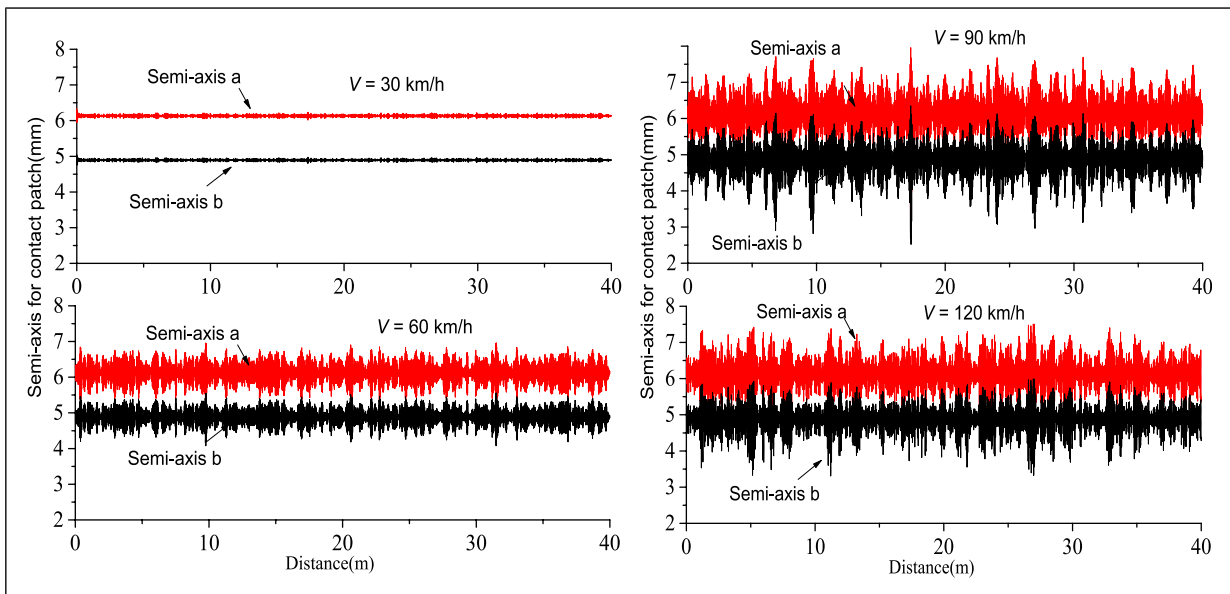


**Figure 9.** Semi-axis for contact patch calculated by the vehicle–track dynamic model when the wheel–rail system was excited by field tested rail irregularity with wavelength of 30–65 mm.

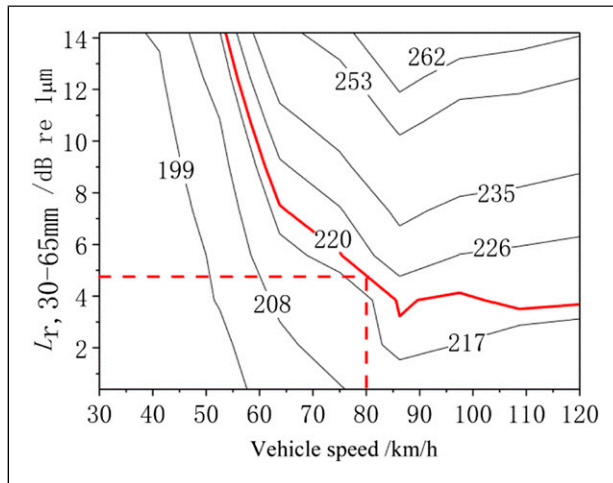
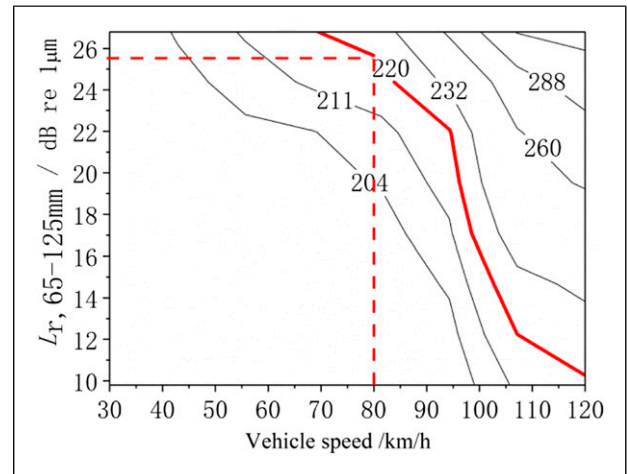
and the fatigue parameters of the left and right wheels of the first wheelset are equivalent. Therefore, the subsequent analysis is for the first wheelset. The influence of the train speed on fatigue parameters (corrugation wavelength 30–65 mm and average roughness level 8.4 dB re 1  $\mu\text{m}$ ) is

considerable, and especially when the speed is larger than 70 km/h, there is a possibility that cracks initiate within the wheel material.

Figure 10 presents the influences of speed and 30–65 mm corrugation on wheel subsurface material fatigue

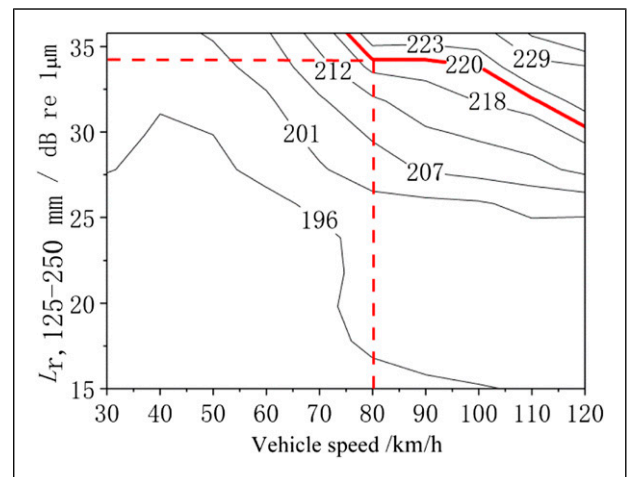
**Table 3.** Fatigue parameters of vehicle front bogie wheel material (unit: MPa).

Train speed	Left wheel of 1st wheelset		Right wheel of 1st wheelset		Left wheel of 2nd wheelset		Right wheel of 2nd wheelset	
	Fatigue parameter	>220(%)	Fatigue parameter	>220 (%)	Fatigue parameter	>220(%)	Fatigue parameter	>220(%)
30	193.8	0	193.9	0	193.7	0	193.7	0
40	194.9	0	195.0	0	194.8	0	194.9	0
50	200.8	0	201.0	0	200.0	0	200.2	0
60	216.4	0	217.0	0	214.1	0	214.6	0
70	229.7	0.5	230.6	0.6	225.3	0.1	226.1	0.2
80	231.4	1	232.2	1.1	228.9	0.5	229.7	0.6
90	247.5	2.6	248.5	2.8	245.0	2	246.1	2.2
100	233.5	2.1	234.5	2.4	232.4	1.7	233.3	1.9
110	236.1	1.6	237.0	1.8	231.3	1.1	232.2	1.3
120	233.5	1.2	234.4	1.3	232.5	0.9	233.4	1.1

**Figure 10.** Influence of vehicle speed and corrugation level of 30–65 mm wavelength on wheel subsurface fatigue.**Figure 11.** Influence of vehicle speed and corrugation level of 65–125 mm wavelength on wheel subsurface fatigue.

parameters. In the figure, contour lines represent the fatigue parameters which are obtained in the different speeds of vehicle and roughness level of 30–65-mm corrugation. Based on the figure, it is found that when the operation speed is smaller than 60 km/h, for example, at sharp curves, the roughness level should be below 9.4 dB re 1  $\mu\text{m}$ , and lower than 5.4 dB re 1  $\mu\text{m}$  at speeds of 60–80 km/h when at shallow curves or on straight lines. For the metro lines with a designed speed of 120 km/h and the actual operation speed between 90–120 km/h, the roughness level within the concerned wavelength range should be less than 4.4 dB re 1  $\mu\text{m}$ , except for the structural resonances are excited such as in the figure at speed of 90 km/h. In the standard of EN ISO 3095–2013 (2013), the ultimate averaging roughness level within 30–65 mm is 2.78 dB re 1  $\mu\text{m}$ .

Figure 11 illustrates the influence of corrugation on fatigue parameters at the wheel subsurface within the

**Figure 12.** Influence of vehicle speed and corrugation level of 125–250 mm wavelength on wheel subsurface fatigue.

**Table 4.** Corrugation level limits for rail grinding of metro lines (unit: dB re 1  $\mu\text{m}$ ).

Wavelength range	Speed		
	60–80 km/h	$\leq 60$ km/h	80–120 km/h
30–65 mm	9.4	5.4	4.4
65–125 mm	26.8	24.8	9.8
125–250 mm		33.8	29.8

wavelength range of 65–125 mm under different speeds. At speed lower than 60 km/h, for example, small radius curving, the corrugation level should be controlled at 26.8 dB re 1  $\mu\text{m}$ ; at the speed of 60–80 km/h, for example, with large curves negotiation, the corrugation level should be within 24.8 dB re 1  $\mu\text{m}$ ; and when the speed is 90–120 km/h, the level is 9.8 dB re 1  $\mu\text{m}$ . From the figure, it is seen that the speed influence on wheel material fatigue caused by corrugation within the wavelength range of 65–125 mm is significant. In the standard, the defined roughness level is 8.32 dB re 1  $\mu\text{m}$ .

Figure 12 shows the influence of corrugation on the fatigue parameters at the wheel subsurface within the wavelength range of 125–250 mm under different speeds. When train speed is smaller than 60 km/h, for example, during curving, the influence is less pronounced. When the speed increases to 80 km/h, corrugation levels in the wavelength range should be controlled below 33.8 dB re 1  $\mu\text{m}$ . When the speed is 90–120 km/h, the upper corrugation level should be 29.8 dB re 1  $\mu\text{m}$ . In the current standard (ISO 3095–2013, 2013), the definition of corrugation level control with wavelength of 125–250 mm is 13.82 dB re 1  $\mu\text{m}$ .

## 5. Discussions

Based on the metro vehicle–track dynamic model and the wheel material fatigue model, the corrugation limit regulations of the current metro rail system are summarized in Table 4. Longer wavelength corrugation shows less influences on wheel material fatigues. However, it has to point out that the wheel–rail rolling noise caused by wheel–rail surface roughness is not considered. Hence, the estimated corrugation limits based on the wheel material fatigue model could be larger when the surface roughness is considered. Besides, the wheel–rail surface roughness, especially short-pitch corrugation, is dominant in the wheel–rail rolling contact noise, which is the main component of the vehicle–track system noise, and the most influential noise source to the surroundings. Therefore, wheel–rail rolling contact noise analysis will be considered in future research. With the consideration of standards on train running safety, wheel–rail rolling contact fatigue, and wheel–rail rolling contact noise, the

control of rail corrugation through rail grinding will be further optimized. Finally, based on the actual operation regulations of a specific line, the grinding criterion applied to the line can be obtained. The methodology presented in this study can be applied to wheel out-of-roundness (Tao et al., 2020).

## 6. Conclusions

This study comprehensively investigates the worldwide standards on corrugation limit control and grinding criterion. By using the field measured corrugation from different track structures, together with a coupled metro vehicle–track dynamic model and a rolling contact fatigue model, some research on the rail grinding criterion is investigated from the aspect of the wheel material fatigue failures. Some summaries are concluded as follows:

1. Currently, it is suggested to grind corrugation based on its wavelength and the actual operation speed.
2. Based on the wheel material fatigue failure criterion, longer corrugation wavelength has less influences on wheel material fatigue.
3. From the study, for metros with a maximum operating speed of 80 km/h, the levels of corrugations with wavelengths of 30–65 mm, 65–125 mm, and 125–250 mm should be smaller than 5.4 dB, 24.8 dB, and 33.8 dB re 1  $\mu\text{m}$ , respectively. For those with the operating speed of 80–120 km/h, the corresponding corrugation levels should be smaller than 4.4 dB, 9.8 dB, and 29.8 dB re 1  $\mu\text{m}$ .

## Declaration of conflicting interests

The author(s) declared no potential conflicts of interest with respect to the research, authorship, and/or publication of this article.

## Funding

The author(s) disclosed receipt of the following financial support for the research, authorship, and/or publication of this article: The present work is supported by the Sichuan Science and Technology Program of China (Grant numbers 2019YFH0053 and 2020YFQ0024), the National Natural Science Foundation of China (Grant number 52002343) and the Routine Science and Technology Assistance Program of China (Grant number KY201701001).

## Data availability statement

The data used to support the findings of this study are available from the corresponding author upon request.

## ORCID iD

Hongqin Liang  <https://orcid.org/0000-0002-5252-7862>

## References

- Auersch L (2020) Simple and fast prediction of train-induced track forces, ground and building vibrations. *Railway Engineering Science* 28(3): 232–250.
- Batten RD, Bellette PA, Meehan PA, et al. (2011) Field and theoretical investigation of the mechanism of corrugation wavelength fixation under speed variation. *Wear* 271: 278–286.
- Bellette PA, Meehan PA, Daniel WJT (2008) Effects of variable pass speed on wear-type corrugation growth. *Journal of Sound and Vibration* 314: 616–634.
- Christophe C, Mihaita H, Andre P (2009) Rotational vibration absorber for the mitigation of rail rutting corrugation. *Vehicle System Dynamics* 47: 641–659.
- Desimone H, Bernasconi A, Beretta S (2006) On the application of Dang Van criterion to rolling contact fatigue. *Wear* 260: 567–572.
- EN 15610:2009 (2009) Railway applications—noise emission—rail roughness—measurement related to rolling noise generation.
- EN 13231–3:2012 (2012) Railway applications—track—acceptance of works—part 3 acceptance of reprofiling rails in track.
- Ekberg A, Kabo E, Andersson H (2002) An engineering model for prediction of rolling contact fatigue of railway wheels. *Fatigue & Fracture of Engineering Materials & Structures* 25: 899–909.
- Eadie DT, Kalousek J, Chiddick KC (2002) The role of high positive friction (HPF) modifier in the control of short pitch corrugations and related phenomena. *Wear* 253: 185–192.
- Eadie DT, Santoro M (2006) Top-of-rail friction control for curve noise mitigation and corrugation rate reduction. *Journal of Sound and Vibration* 293: 747–757.
- Eadie DT, Santoro M, Oldknow K, et al. (2008) Field studies of the effect of friction modifiers on short pitch corrugation generation in curves. *Wear* 265: 1212–1221.
- Grassie SL (2009) Rail corrugation: characteristics, causes, and treatments. *Proceedings of the Institution of Mechanical Engineers, Part F: Journal of Rail and Rapid Transit* 223: 581–596.
- General Railway Transport (2014) *Management Measures for Rail Grinding of High-Speed Railway*. Beijing: China Railway Corporation.
- Guidat A (1996) The fundamental benefits of preventive rail grinding. *Rai Engineering Journal*.
- Gullers P, Andersson L, Lundén R (2008) High-frequency vertical wheel-rail contact forces-field measurements and influence of track irregularities. *Wear* 265: 1472–1478.
- Grassie SL, Elkins JA. (1998) Rail corrugation on North American transit systems. *Vehicle System Dynamics* 29: 5–17.
- Grassie SL, Kalousek J (1993) Rail corrugation: characteristics, causes and treatments. *Proceedings of the Institution of Mechanical Engineers, Part F: Journal of Rail and Rapid Transit* 207: 57–68.
- Grassie SL, Saxon MJ, Smith JD (1999) Measurement of longitudinal rail irregularities and criteria for acceptable grinding. *Journal of Sound and Vibration* 227: 949–964.
- Heyder R, Girsch G (2005) Testing of HSH rails in high-speed tracks to minimise rail damage. *Wear* 258: 1014–1021.
- Hiensch M (2002) Rail corrugation in the Netherlands—measurements and simulations. *Wear* 253: 140–149.
- ISO 3095–2013 (2013) *Acoustics—Railway Applications—Measurement of Noise Emitted by Railbound Vehicles*.
- Jin XS, Wen ZF, Wang KY (2005) Effect of track irregularities on initiation and evolution of rail corrugation. *Journal of Sound and Vibration* 285: 121–148.
- Jin XS, Li W, Wen ZF, et al. (2016) An investigation into rail corrugation, its mechanisms and effects on the dynamic behavior of metro trains and tracks in China. *International Journal of Railway Technology* 5(3): 1–29.
- Li W, Wang H, Wen Z, et al. (2016) An investigation into the mechanism of metro rail corrugation using experimental and theoretical methods. *Proceedings of the Institution of Mechanical Engineers, Part F: Journal of Rail and Rapid Transit* 230: 1025–1039.
- Li S, Li Z, Núñez A, et al. (2017) New insights into the short pitch corrugation enigma based on 3D-FE coupled dynamic vehicle-track modeling of frictional rolling contact. *Applied Sciences* 7: 807.
- Li W (2015) *Study on Root Cause of Metro Rail Corrugation and its Influence on Behavior of Vehicle-Track system*. PhD Thesis, Southwest Jiaotong University, Chengdu, China.
- Meehan PA, Bellette PA, Batten RD, et al. (2009) A case study of wear-type rail corrugation prediction and control using speed variation. *Journal of Sound and Vibration* 325: 85–105.
- Nielsen JCO and Ekberg A (2011) Acceptance criterion for rail roughness level spectrum based on assessment of rolling contact fatigue and rolling noise. *Wear* 271: 319–327.
- Railway Transport (2006) *Rules for Maintenance of Railway Lines*. Beijing: Ministry of Railways.
- Tao G, Wen Z, Jin X, et al. (2020) Polygonisation of railway wheels: a critical review. *Railway Engineering Science* 28(4): 317–345.
- TB/T 3095–2013 (1994) *Test Method and Evaluation Standard for Dynamic Performance of Railway Locomotives*. Beijing: Ministry of Railways.
- TB/T 2489–94 (1995) *Wheel-rail Horizontal Force and Vertical Force Ground Test Method*. Beijing: Ministry of Railways.
- TB/T 2489–94 (2010) *Public Works—Part 22: Rails/turnout Grinding Operations*. Beijing: Ministry of Railways.
- Wu TX (2011) Effects on short pitch rail corrugation growth of a rail vibration absorber/damper. *Wear* 271: 339–348.
- Xu L, Zhai W (2020) Train-track coupled dynamics analysis: system spatial variation on geometry, physics and mechanics. *Railway Engineering Science* 28(1): 36–53.
- Zhai W (2020) *Vehicle-track Coupled Dynamics Theory and Applications*. Singapore: Springer.